2007 IEEE International Conference on
Robotics and Automation
Roma, Italy, 10-14 April 2007

Accuracy of Kinematic and Dynamic Models of a Gantry-Tau Parallel Kinematic Robot

Isolde Dressler, Anders Robertsson and Rolf Johansson

Abstract— **In this article, a new kinematic and a dynamic model for a 3-degree-of-freedom Gantry-Tau parallel kinematic robot are presented. Similar to an earlier proposed kinematic model, the dynamic model is based on the assumption of parallel actuator axes and constant end-effector orientation. The new kinematic model takes into account rotations of actuator axes which do not affect the end-effector orientation. Results from a calibration experiment show an improved positioning accuracy of the new kinematic model. A more general model of the robot including possible geometric inaccuracies causing deviations from the model assumptions has been developed in the modeling language Modelica. In a simulation, the proposed dynamic model is tested as a feedforward term in a control application and is found to improve the tracking performance considerably.**

I. INTRODUCTION

Today industrial robots are widely used in large enterprises within large-scale production. To strengthen the competitiveness of small- and medium-sized enterprises (SMEs), new modular robots are needed, which can be used flexibly for changing applications [10]. This kind of robot concept might include assembly of the robot at the manufacturing site. Parallel kinematic manipulators (PKMs) gain in importance in the field of industrial robotics and outperform serial structures in accuracy, speed and structural stiffness [11]. The Gantry-Tau parallel kinematic robot [1] is one approach to find a robot suitable for SME applications. Its actuators can be reconfigured according to a specific application. The robot has a larger workspace compared to most parallel manipulators [1]. The modularity of the robot and the possible robot assembly and reconfiguration by SME staff may lead to kinematic errors which decrease the positioning accuracy. Therefore, an accurate kinematic model able to cope with potential assembling errors is needed. High speed control [12] requires an accurate dynamic model of the manipulator.

The Gantry-Tau parallel robot (Fig. 1) is a Gantry variant of the 3-degree-of-freedom (DOF) Tau parallel robot [4] which is based on an ABB patent [5]. Two different variants of the Gantry-Tau PKM have been presented with constant [1] and variable [2] end-effector orientation. Kinematic errors have been studied for the Tau parallel robot [4] and the Gantry-Tau PKM with variable end-effector orientation [3]. A dynamic model of the Tau PKM was presented in [6].

This work has been funded by the European Comission's Sixth Framework Programme under grant no.011838 as part of the Integrated Project SMErobot™.

Isolde Dressler, Anders Robertsson and Rolf Johansson are with Department of Automatic Control, LTH, Lund University, SE-221 00 Lund, Sweden, isolde.dressler@control.lth.se

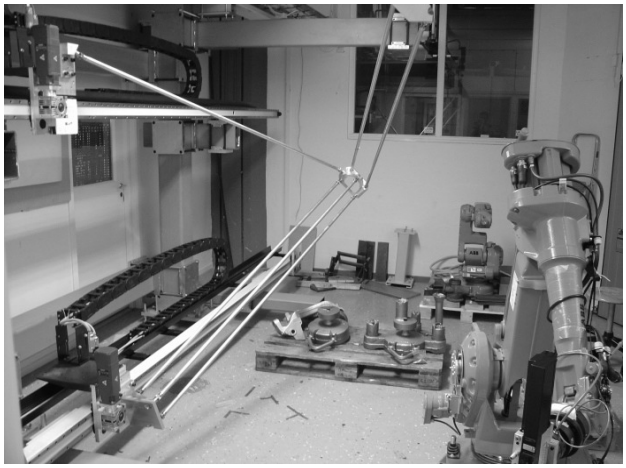

Fig. 1. A prototype of a Gantry-Tau PKM (in the left of the picture) at the Robotics Lab at LTH, Lund University

In this paper, a kinematic model for the Gantry-Tau PKM with constant end-effector orientation is proposed which takes into account one kind of kinematic errors. A dynamic model for the same manipulator is proposed as well. The accuracy of the new kinematic model compared to the earlier proposed model is studied in a calibration experiment. The dynamic model is tested as a feedforward term in a control application by simulation.

The article is organized as follows: In Section II, the proposed kinematic and dynamic models are presented. Section III presents experiment and simulation results including the comparison of the two kinematic models in a calibration experiment and the evaluation of the dynamic model in a control application. The results are discussed in Section IV before concluding in Section V.

II. KINEMATIC AND DYNAMIC MODELING

A. Nominal Kinematic Model

The Gantry-Tau robot (Fig. 1) consists of three kinematic chains. Each kinematic chain includes a prismatic actuator which is connected to the end-effector plate via a link cluster. The prismatic joints are implemented as carts moving on tracks. The altogether six links are distributed to the clusters in a 3-2-1 configuration. They are connected to the actuator carts and end-effector plate via passive spherical joints. The placement of the joints on carts and end-effector plate in the Tau-configuration is such that links belonging to one cluster form parallelograms, which assures a constant end-effector orientation.

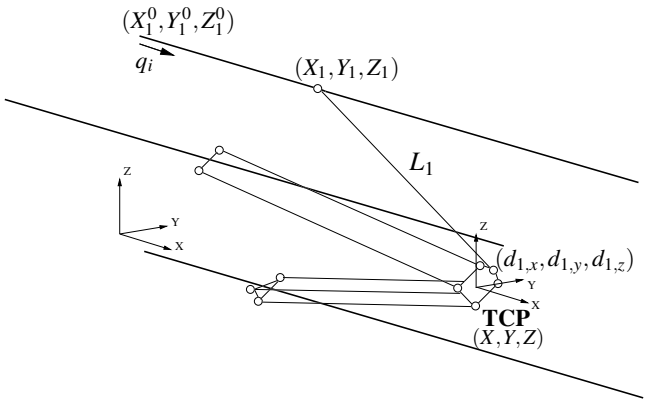

Fig. 2. Schematic Gantry-Tau PKM with parameter and variable notation exemplified on track 1; all coordinates are given in global frame except the joint position on the end-effector plate, which is given in TCP coordinates

Fig. 2 shows the used notation for geometric parameters and variables. Tracks and link clusters are numbered according to the number of links in the kinematic chain. Two different coordinate frames are used: the global frame and a coordinate system which has the same orientation but whose origin is located in the tool center point (TCP). It is assumed that the zero position of the articular coordinates q_i corresponds to $X_i = 0$ and that the actuator axes are parallel to the x-axis, so that $q_i = X_i$.

Thanks to the Tau-configuration, the orientation of the end-effector plate is constant and the 3 DOFs of the robot are completely translational, so it is sufficient to consider one link per link cluster. The closure equation for link i is then [1]:

$$L_i^2 - (\Delta X_i^2 + \Delta Y_i^2 + \Delta Z_i^2) = 0, \tag{1}$$

where $(\Delta X_i, \Delta Y_i, \Delta Z_i)^T$ is the vector along link i:

$$\begin{aligned} \Delta X_i &= X + d_{i,x} - X_i \\ \Delta Y_i &= Y + d_{i,y} - Y_i \\ \Delta Z_i &= Z + d_{i,z} - Z_i \end{aligned} \tag{2}$$

For the inverse kinematic problem, the equations are solved for the articular coordinates $q_1 = X_1$, $q_2 = X_2$ and $q_3 = X_3$, which can be done independently for each actuator. The direct kinematics problem consists in solving the equations for the TCP position $(X, Y, Z)^T$, which can be done through a stepwise geometric solution [1] or with the aid of a symbolic computation tool, e.g. Maple.

For the direct kinematic problem, two solutions exist, the end-effector can be on either side of the actuators. For the inverse kinematic problem, for each link cluster two solutions exist, altogether $2^3 = 8$ solutions. When using the kinematic model for control, a configurations state has to decide which one of the solutions is desired.

B. Kinematic Model for Nonparallel Actuator Axes

Assuming an arbitrary orientation of track i (Fig. 3), the current cart i position $(X_i, Y_i, Z_i)^T$ in (2) can be expressed as:

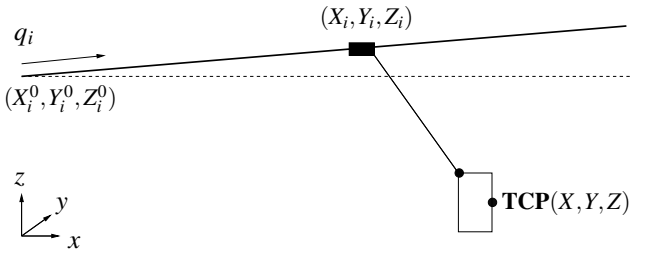

Fig. 3. Illustration of (3): track with orientation error and fictive track parallel to x-axis (dashed)

$$\begin{pmatrix} X_i \\ Y_i \\ Z_i \end{pmatrix} = \begin{pmatrix} 0 \\ Y_i^0 \\ Z_i^0 \end{pmatrix} + \begin{pmatrix} c_{i,x} \\ c_{i,y} \\ c_{i,z} \end{pmatrix} q_i, \tag{3}$$

where $(c_{i,x}, c_{i,y}, c_{i,z})^T$ is the unit vector along the rotated track in positive q_i direction.

Compared to the case for parallel actuator axes, ΔX_i, ΔY_i and ΔZ_i in (1) and (2) are now dependent on the articular coordinate q_i instead of only ΔX_i. That makes the solution of inverse and direct kinematics more complex, but it is anyhow possible to solve the inverse kinematic problem with a symbolic computation tool. The stepwise geometric method [1] can be applied to solve the direct kinematic problem if the cart positions are modified according to (3). Inverse kinematics can still be solved independently for each actuator. Explicit solutions of the quadratic equations are not cited here for space reasons.

The inverse and direct kinematic problems have the same number of solutions as in the case of parallel articulator axes, 2 for the direct kinematics and 8 for the inverse kinematics.

The above kinematic model is based on the fact that the orientation of the end-effector is constant which is equivalent to that all links belonging to one cluster form parallelograms. When a robot constructed for parallel articulator axes is assembled imprecisely and tracks are slightly nonparallel relative to each other, this will mostly not be the case. Only track orientations which do not twist the link cluster will assure constant end-effector orientation.

Even if the resulting end-effector orientation is constant, it might not be the intended one. Another interesting point is that rotation around the x-axis does not influence the kinematics solution. Only the movement of the spherical joint on the cart is important, but not how the track is oriented around it. If only q_1, q_2, q_3 and (X, Y, Z) data are used for calibration, it might not be possible to identify the orientation of the platform perfectly. For the case of the prototype at LTH (Fig. 1) however, a small rotation around the z-axis is the most likely deviation, and a rotation around the x-axis is nearly impossible.

Not all tracks affect the end-effector orientation, link cluster 1 has no influence on it and link cluster 3 is most important; it determines the orientation of the plane formed by its joints on the end-effector plate.

C. A Dynamic Model

The dynamic model of the Gantry-Tau PKM is based on the assumption that the actuator axes are parallel to each other. Carts, links and end-effector plate are modeled by point masses in their center of gravity. A link cluster is represented by one link with the mass of all links in the cluster. The joints are massless, but their masses can be included in the carts' and the end-effector plate's masses.

The dynamic model was derived by extracting the model equations from a Modelica model of the Gantry-Tau robot. Modelica is an object-oriented modeling language, which is efficient in modeling multi-domain complex systems. The Modelica MultiBody Library [9] facilitates the modeling of rigid body systems. Joints and bodies can intuitively be connected to construct a mechanism. It models kinematics and dynamics for rigid bodies, which are considered as point masses. It does not take into account elasticities or friction. Dymola by Dynasim [8], a software tool to create and simulate Modelica models, allows to export the system equations of a model together with expressions to calculate redundant variables. After some variable and parameter changes the equations could be expressed in terms of the desired variables and parameters. The original Modelica model involved about 4000, partially redundant variables.

The equations relevant for the dynamic model are force balances with respect to actuator forces over carts 1, 2 and 3 (x direction) and the end-effector plate (x, y and z direction). Gravity points in negative z direction, f_i are auxiliary force variables, that is to say the constraint forces in direction of the link:

$$\tau_i = m_{c,i}\ddot{X}_i + \frac{m_{a,i}}{4}(\ddot{X}+\ddot{X}_i) - \Delta X_i S_i + \frac{\Delta X_i}{L_i} f_i \tag{4}$$

$$0 = m_p \ddot{X} + \sum_{i=1}^{3}\left(\frac{m_{a,i}}{4}(\ddot{X}+\ddot{X}_i) + \Delta X_i S_i - \frac{\Delta X_i}{L_i} f_i\right) \tag{5}$$

$$0 = m_p \ddot{Y} + \sum_{i=1}^{3}\left(\frac{m_{a,i}}{4}\ddot{Y} + \Delta Y_i S_i - \frac{\Delta Y_i}{L_i} f_i\right) \tag{6}$$

$$0 = m_p(\ddot{Z}+g) + \sum_{i=1}^{3}\left(\frac{m_{a,i}}{2}(\frac{\ddot{Z}}{2}+g) + \Delta Z_i S_i - \frac{\Delta Z_i}{L_i} f_i\right) \tag{7}$$

where $m_{c,i}$, $m_{a,i}$ and m_p are the masses of cart i, link cluster i and end-effector plate, respectively, τ_i the actuator forces and

$$S_i = \frac{m_{a,i}}{2}\frac{1}{L_i^2}\left(\Delta X_i\frac{\ddot{X}+\ddot{X}_i}{2} + \Delta Y_i\frac{\ddot{Y}}{2} + \Delta Z_i(\frac{\ddot{Z}}{2}+g)\right)$$

Solving (4) for f_i for $i = 1,2,3$ and inserting the solutions into (5) – (7) gives:

$$\sum_{i=1}^{3}\tau_i = m_p\ddot{X} + \sum_{i=1}^{3}\left(m_{c,i}\ddot{X}_i + \frac{m_{a,i}}{2}(\ddot{X}+\ddot{X}_i)\right) \tag{8}$$

$$\sum_{i=1}^{3}\frac{\Delta Y_i}{\Delta X_i}\tau_i = m_p(\ddot{Y}+g) + \sum_{i=1}^{3}\left(m_{c,i}\frac{\Delta Y_i}{\Delta X_i}\ddot{X}_i + \frac{m_{a,i}}{4}\frac{\Delta Y_i}{\Delta X_i}(\ddot{X}+\ddot{X}_i) + \frac{m_{a,i}}{2}(\frac{\ddot{Y}}{2}+g)\right) \tag{9}$$

$$\sum_{i=1}^{3}\frac{\Delta Z_i}{\Delta X_i}\tau_i = m_p\ddot{Z} + \sum_{i=1}^{3}\left(m_{c,i}\frac{\Delta Z_i}{\Delta X_i}\ddot{X}_i + \frac{m_{a,i}}{4}\frac{\Delta Z_i}{\Delta X_i}(\ddot{X}+\ddot{X}_i) + \frac{m_{a,i}}{4}\ddot{Z}\right) \tag{10}$$

In matrix form:

$$M_1\begin{pmatrix}\ddot{X}_1\\ \ddot{X}_2\\ \ddot{X}_3\end{pmatrix} + M_2\begin{pmatrix}\ddot{X}\\ \ddot{Y}\\ \ddot{Z}\end{pmatrix} + G = J^{-T}\begin{pmatrix}\tau_1\\ \tau_2\\ \tau_3\end{pmatrix} \tag{11}$$

with

$$M_1 = \begin{pmatrix} M_1(:,1) & M_1(:,2) & M_1(:,3)\end{pmatrix},$$

$$M_1(:,i) = \begin{pmatrix} m_{c,i} + \frac{m_{a,i}}{2} \\ \frac{\Delta Y_i}{\Delta X_i}(m_{c,i} + \frac{m_{a,i}}{4}) \\ \frac{\Delta Z_i}{\Delta X_i}(m_{c,i} + \frac{m_{a,i}}{4})\end{pmatrix},$$

$$M_2 = \begin{pmatrix} m_p + \frac{\sum_{i=1}^{3} m_{a,i}}{2} & \cdots & \\ \sum_{i=1}^{3}\frac{m_{a,i}}{4}\frac{\Delta Y_i}{\Delta X_i} & \cdots & \\ \sum_{i=1}^{3}\frac{m_{a,i}}{4}\frac{\Delta Z_i}{\Delta X_i} & \cdots & \end{pmatrix}$$

$$\begin{pmatrix} 0 & 0 \\ m_p + \frac{\sum_{i=1}^{3} m_{a,i}}{4} & 0 \\ 0 & m_p + \frac{\sum_{i=1}^{3} m_{a,i}}{4}\end{pmatrix},$$

$$G = g\begin{pmatrix} 0 \\ \frac{m_{a,1}+m_{a,2}+m_{a,3}}{2} + m_p \\ 0\end{pmatrix},$$

and the transposed inverse kinematic Jacobian matrix

$$J^{-T} = \begin{pmatrix} 1 & 1 & 1 \\ \frac{\Delta Y_1}{\Delta X_1} & \frac{\Delta Y_2}{\Delta X_2} & \frac{\Delta Y_3}{\Delta X_3} \\ \frac{\Delta Z_1}{\Delta X_1} & \frac{\Delta Z_2}{\Delta X_2} & \frac{\Delta Z_3}{\Delta X_3}\end{pmatrix} \tag{12}$$

The end-effector acceleration is obtained by differentiating the closure equations twice by time, or alternatively the relation can be obtained from the Modelica model in the same way as the dynamic model:

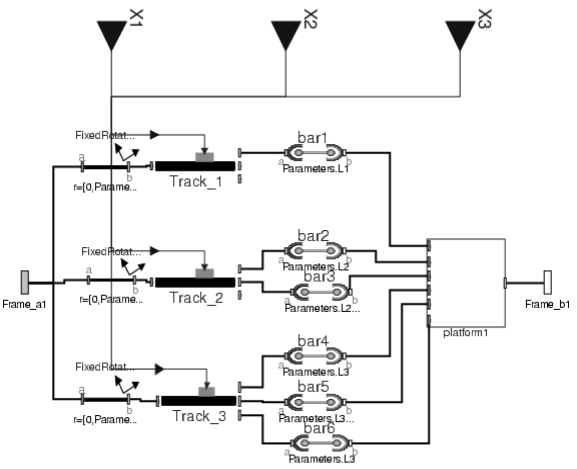

Fig. 4. Modelica model of a Gantry-Tau PKM with geometric inaccuracies

$$\begin{pmatrix} \ddot{X} \\ \ddot{Y} \\ \ddot{Z} \end{pmatrix} = J \begin{pmatrix} \ddot{X}_1 \\ \ddot{X}_2 \\ \ddot{X}_3 \end{pmatrix} - \begin{pmatrix} \Delta X_1 & \Delta Y_1 & \Delta Z_1 \\ \Delta X_2 & \Delta Y_2 & \Delta Z_2 \\ \Delta X_3 & \Delta Y_3 & \Delta Z_3 \end{pmatrix}^{-1} \cdot \begin{pmatrix} (\dot{X}-\dot{X}_1)^2+\dot{Y}^2+\dot{Z}^2 \\ (\dot{X}-\dot{X}_2)^2+\dot{Y}^2+\dot{Z}^2 \\ (\dot{X}-\dot{X}_3)^2+\dot{Y}^2+\dot{Z}^2 \end{pmatrix} \quad (13)$$

The end-effector velocity can be obtained by inverting the inverse Jacobian matrix from (12):

$$\begin{pmatrix} \dot{X} \\ \dot{Y} \\ \dot{Z} \end{pmatrix} = J \begin{pmatrix} \dot{X}_1 \\ \dot{X}_2 \\ \dot{X}_3 \end{pmatrix} \quad (14)$$

D. A General Modelica Model

Fig. 4 shows a picture of the Modelica model of the Gantry-Tau PKM. The actuator tracks can be placed and oriented arbitrarily as long as a solution of the kinematic problem exists. The lengths of all 6 bars can be defined independently and the placement of joints on carts and end-effector plate is arbitrary. The inertia of the robot is modeled by point masses associated with carts, links and end-effector plate. The mass of the joints can be included in plate and carts.

The values of geometric and mass parameters are adapted to the prototype at LTH (Fig. 1). Compared to the ideal Gantry-Tau robot, track 1 and 2 have been rotated around the z-axis with 1° and -1° respectively. The magnitude of 1° seems a reasonable maximum error for real applications. For one of the links belonging to cluster 2 and 3, respectively, it has been assumed that their lengths are 5 mm too long and too short respectively. This would be a quite extreme manufacturing error in reality.

III. EXPERIMENT AND SIMULATION RESULTS

A. Kinematic Models

In a calibration experiment, the accuracy of the two different kinematic models was compared. The Gantry-Tau prototype at LTH was calibrated with the aid of a Leica laser tracker. The tracks of this prototype deviate, as earlier measurements have shown, around 0.1° from being parallel to each other.

TABLE I

CALIBRATION RESULTS FOR THE TWO KINEMATIC MODELS

Description	parallel	nonparallel
$L_1(m)$	2.0613	2.0608
$-d_{1,x}(m)$	-1.8093	-1.8089
$Y_1^0 - d_{1,y}(m)$	3.5095	3.5093
$Z_1^0 - d_{1,z}(m)$	0.0040631	0.0038717
$c_{1,x}$	–	0.99935
$c_{1,y}$	–	-0.029265
$c_{1,z}$	–	-0.0021529
$L_2(m)$	2.0662	2.0633
$-d_{2,x}(m)$	-1.8688	-1.8656
$Y_2^0 - d_{2,y}(m)$	2.2455	2.2456
$Z_2^0 - d_{2,z}(m)$	0.20754	0.20735
$c_{2,x}$	–	0.99901
$c_{2,y}$	–	-0.026378
$c_{2,z}$	–	-0.0044864
$L_3(m)$	2.0632	2.0611
$-d_{3,x}(m)$	-1.8109	-1.8086
$Y_3^0 - d_{3,y}(m)$	3.2774	3.2774
$Z_3^0 - d_{3,z}(m)$	-1.4436	-1.4434
$c_{3,x}$	–	0.99966
$c_{3,y}$	–	-0.029618
$c_{3,z}$	–	-0.0013514
V_1	$9.2981 \cdot 10^{-5}$	$7.2422 \cdot 10^{-5}$
V_2	$8.1309 \cdot 10^{-4}$	$7.4559 \cdot 10^{-5}$
V_3	$5.8639 \cdot 10^{-4}$	$3.4325 \cdot 10^{-5}$

With the laser tracker, 779 TCP poses of the Gantry-Tau prototype have been recorded. The robot workspace has been divided into 12 layers on which an equal pattern of measurements has been taken. Instead of measuring the cart positions as well, their reference values were used.

Table I shows the results of the kinematic calibration. Each of the three kinematic chains was calibrated separately by using every second measurement, so that the measurement points were well distributed over the workspace. The closure equations of the models were used as cost function V for minimization:

$$V_i = \sum_{k=1}^{N} \left(L_i^2 - (\Delta X_{i,k}^2 + \Delta Y_{i,k}^2 + \Delta Z_{i,k}^2) \right) \quad (15)$$

where $\Delta X_{i,k}$, $\Delta Y_{i,k}$ and $\Delta Z_{i,k}$ were calculated by inserting the k-th measured TCP and cart i position into (2). For the model with nonparallel tracks, (3) had to be used as well. The minimization was performed by the Matlab function `fminunc` with standard options. For the model with parallel tracks, a mean value of the track directions known from earlier measurements has been used. Not all of the kinematic parameters can be estimated independently, see Table I, as only their difference is included in the closure equation.

The validation of the calibration with the measured poses not used for calibration showed an improved accuracy of the proposed kinematic model. The direct kinematic models were used to compare calculated TCP positions with the measured ones. The absolute positioning errors were mostly

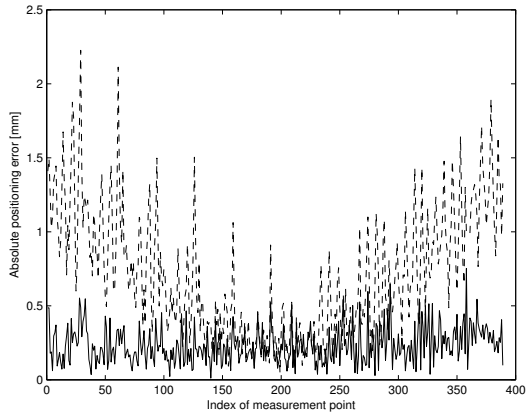

Fig. 5. Absolute positioning error for kinematic model with parallel tracks (dashed) and nonparallel tracks (solid)

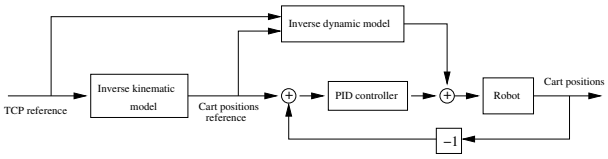

Fig. 6. Block diagram of the controller used in the simulations

smaller that 0.5 mm for the proposed model or mostly smaller than 1.5 mm for the model with parallel tracks (see Fig. 5). The cost functions calculated for the remaining poses were of the same order of magnitude as for the first half of the measurements after minimization.

B. Dynamic Model

In the following simulations, the general Modelica robot model has been controlled to follow a helix-shaped reference trajectory. Fig. 6 gives an overview of the controller structure [13]. An inverse kinematic model generates the reference values for the articular coordinates. The inverse dynamical model derived in Section II-C calculates the required actuator forces. Differences between the cart positions and the corresponding reference value are controlled by a PID controller, which controls each cart independently.

For the inverse kinematic model, the proposed model with nonparallel tracks has been used with the geometric parameters calibrated in the same way as in Section III-A, but with measurements generated by the general Modelica model. The masses for end-effector plate and carts in the inverse dynamic model match exactly those in the robot model; 20 kg for the carts and 10 kg for the end-effector plate. For the links, the same density and diameter was used to calculate the masses, but different link lengths according to calibration results.

Fig. 7 and 8 show the simulation results. In Fig. 7, the cart positions with the corresponding reference values can be seen. After some oscillations in the beginning, the carts follow their reference quite well. The oscillations are due to the fact that the control signal acts as a force directly on

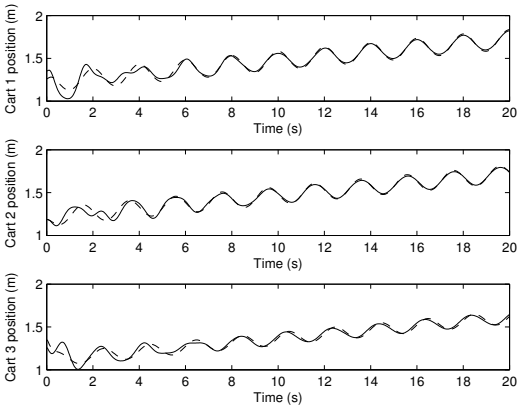

Fig. 7. Reference (dashed) and actual (solid) cart position for carts 1 to 3

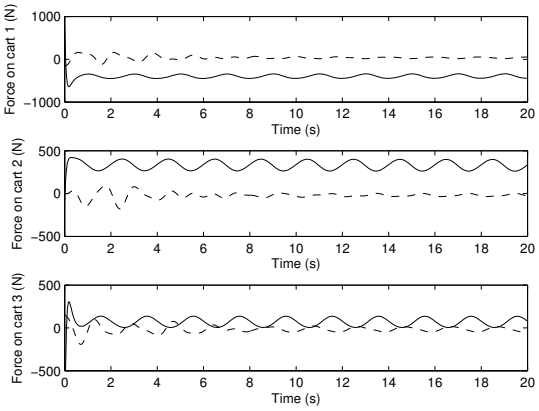

Fig. 8. The two parts of the applied forces on carts 1 to 3: the force calculated by the inverse dynamic model (solid) and the PID controller output signal (dashed); it can be seen that the inverse dynamic model contributes the larger part to the control signal

the cart without any transmission in between, which makes the system very sensitive and hard to control. However, the accuracy of the dynamic model can still be estimated. Fig. 8 shows the two parts of the control signal: the force generated by the PID controller and the force generated by the inverse dynamic model. As the carts follow their reference positions quite well after approximately 5 seconds, the force generated by the PID controller is an estimate of the inverse dynamic model error. After the oscillations in the beginning, the absolute force errors oscillate between 0 and 60 N. The accuracy of the dynamic model depends considerably on the accuracy of the kinematic model; errors in the Jacobian matrix will lead to errors in the calculated force.

IV. DISCUSSION

The calibration experiment showed that the proposed kinematic model has an improved positioning accuracy compared to the earlier known model. The error for the new model has a mean value around 0.23 mm and is mostly smaller than 0.5 mm whereas the model with parallel tracks has a mean

positioning error around 0.7 mm and reaches 2 mm for two measurements.

The decrease of the error for the parallel tracks model in the middle of Figure 5 is due to a better data fit in the middle of the workspace. The track assumed by the model intersects here with the real track.

The use of a more sophisticated optimization algorithm for calibration than the Matlab function `fminunc` with standard options was not part of this study, but the value of the cost function after minimization together with the number of measurement points suggests that no large improvements can be made for the used data.

The accuracy of the dynamic model depends considerably on the accuracy of the kinematic model; as the masses used in the dynamic model were assumed to be perfectly known, the errors are to a large part due to errors in the kinematic model. In a real application, unmodeled features, e.g. friction and actuator dynamics, decrease the accuracy of the dynamic model.

V. CONCLUSIONS AND FUTURE WORK

A kinematic model for a Gantry-Tau PKM was presented which takes into account angular deviations of the tracks. A calibration experiment showed an improvement in accuracy of the new model compared to an ideal kinematic model.

A dynamic model of the same robot has been presented and tested in a simulated control application where it has been used as a feedforward term to generate the actuator forces necessary to follow a reference trajectory. Positioning errors were corrected by a PID controller. The absolute errors of the articulate forces calculated by the inverse dynamic model oscillated between 0 and 60 N.

In the future, the simulation results presented here will be verified on the Gantry-Tau prototype (Fig. 1), which was lacking some of the equipment needed for control experiments when this work was done. In order to get an accurate dynamic model, dynamic calibration of the Gantry-Tau PKM will be done.

VI. ACKNOWLEDGEMENTS

This work has been funded by the European Commission's Sixth Framework Programme under grant no. 011838 as part of the Integrated Project SMErobot™.

REFERENCES

[1] L. Johannesson, V. Berbyuk and T. Brogårdh, "Gantry-Tau – A New Three Degrees of Freedom Parallel Kinematic Robot", *in Parallel Kinematic Machines in Research and Practice; The 4th Chemnitz Parallel Kinematics Seminar*, 2004, pp. 731-734.

[2] T. Brogårdh, S. Hanssen and G. Hovland, "Application-Oriented Development of Parallel Kinematic Manipulators with Large Workspace", *in Proc. of the 2nd International Colloquium of the Collaborative Research Center 562: Robotic Systems for Handling and Assembly*, Braunschweig, Germany, 2005, pp.153-170.

[3] I. Williams, G. Hovland and T. Brogårdh, "Kinematic Error Calibration of the Gantry-Tau Parallel Manipulator", *in Proceedings International Conference on Robotics and Automation*, Orlando, FL, 2006, pp.4199-4204.

[4] H. Cui, Z. Zhu, Z. Gan and T. Brogårdh, "Kinematic analysis and error modeling of TAU parallel robot", *in Robotics and Computer-Integrated Manufacturing*, Vol.21, 2005, pp.497-505.

[5] T. Brogårdh, *A device for relative movement of two elements*, Patent WO 97/33726, 1996.

[6] Z. Zhu, J. Li, Z. Gan and H. Zhang, "Kinematic and dynamic modelling for real-time control of Tau parallel robot", *in Mechanism and Machine Theory*, Vol. 40, 2005, pp. 1051-1067.

[7] Modelica homepage, http://www.Modelica.org/.

[8] Dynasim homepage, http://www.Dynasim.se/.

[9] M. Otter, H. Elmqvist, S.-E. Mattson, "The New Modelica MultiBody Library", *in Proc. of the 3rd International Modelica Conference*, Linköping, Sweden, 2003, pp. 311-330.

[10] SMErobot homepage, http://www.smerobot.org.

[11] J.-P. Merlet, *Parallel Robots*, Kluwer Academic Publishers, Norwell, MA, 2000.

[12] R.M. Murray, Z. Li and S.S. Sastry, *A Mathematical Introduction to Robotic Manipulation*, CRC Press, Boca Raton, FL, 1994.

[13] L. Sciavicco, B. Siciliano, *Modeling and Control of Robot Manipulators*, McGraw Hill, New York, 1996.